GSA Data Repository 2019062

Discovery of vast fluvial deposits provides evidence for drawdown during the late Miocene Messinian salinity crisis

Andrew S. Madof[1], Claudia Bertoni[2], and Johanna Lofi[3]

[1]Chevron Energy Technology Company, Houston, Texas 77002-7308, USA

[2]University of Oxford, Department of Earth Sciences, Oxford OX1 3AN, UK

[3]Université de Montpellier, CNRS, Géosciences Montpellier, Montpellier 34095, France

METHODS

Seismic interpretation

Reflections were mapped on zero-phase full-stack two- and three-dimensional (2-D and 3-D) seismic data in two-way travel time (TWTT), using commercial seismic-interpretation software (SeisEarth® by Paradigm®). High-amplitude peak reflections were used to trace the base and top of the Nahr Menashe deposit (i.e., intermediate erosional surface [IES] and top erosional surface [TES], respectively); the base of evaporitic accumulations was mapped via tracing high-amplitude trough reflections. Thickness maps in TWTT (isochrons) were created for evaporites and the Nahr Menashe via the subtraction of the top and base of the deposits and are displayed in Fig. 3A–3B and Fig. DR3.

Spectral decomposition

Spectral decomposition was calculated on four 3-D volumes using commercial seismic-interpretation software (GeoTeric® by Foster Findlay Associates). The Uniform Constant Q routine was used to maintain an optimal relationship between dominant and bandwidth

frequencies, which resulted in a balance between vertical resolution and frequency resolution, respectively (see Fig. DR4).

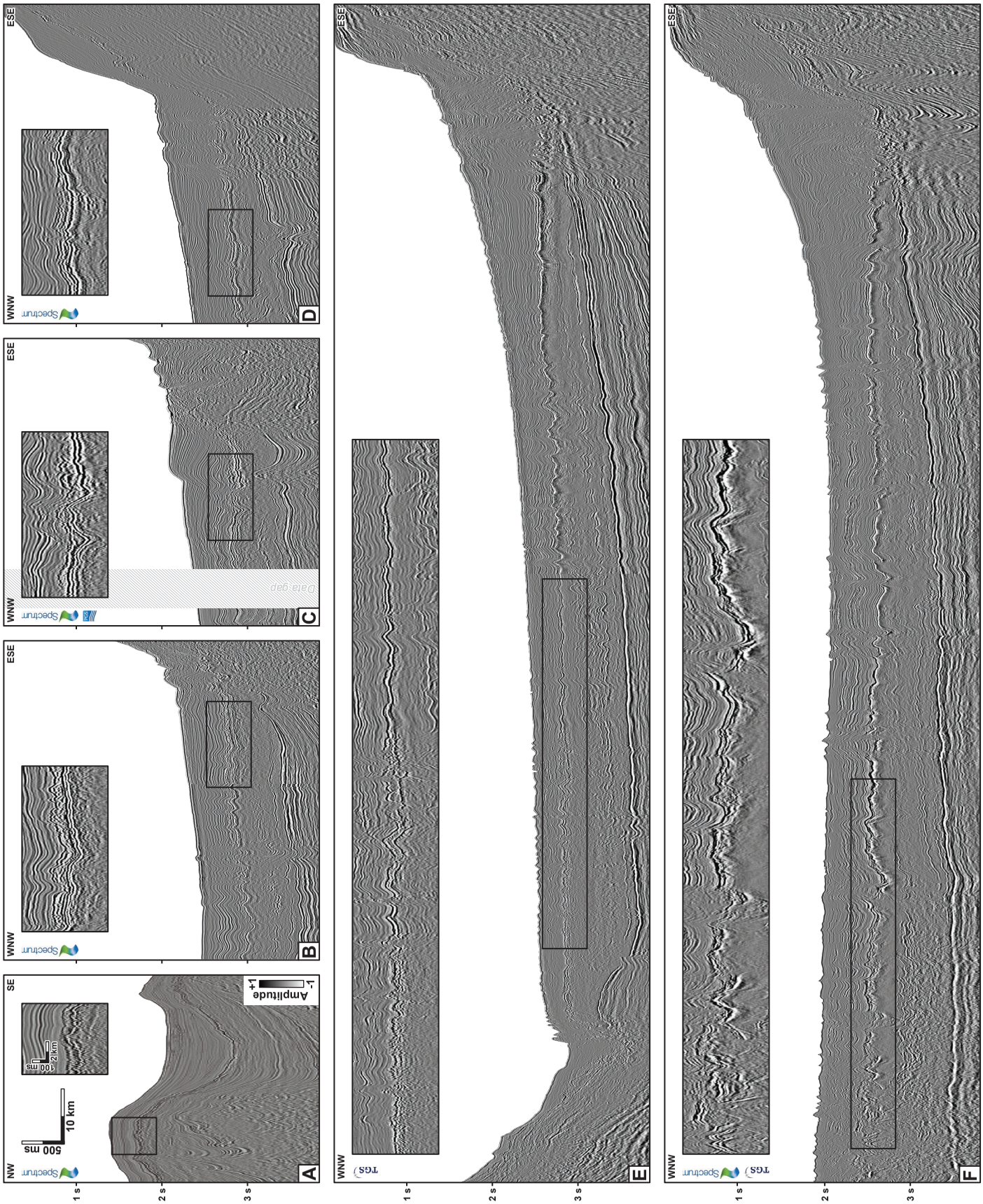

Figure DR1. Uninterpreted 2D seismic lines, showing reflection geometry of the eastern Mediterranean (offshore Cyprus, Syria, Lebanon, and Israel). See Fig. 3A (bottom right) for location map, and Fig. DR2 for interpretation. Scales are the same for all panels. Data courtesy of PGS, Spectrum, TGS, and the Lebanese Ministry of Energy and Water.

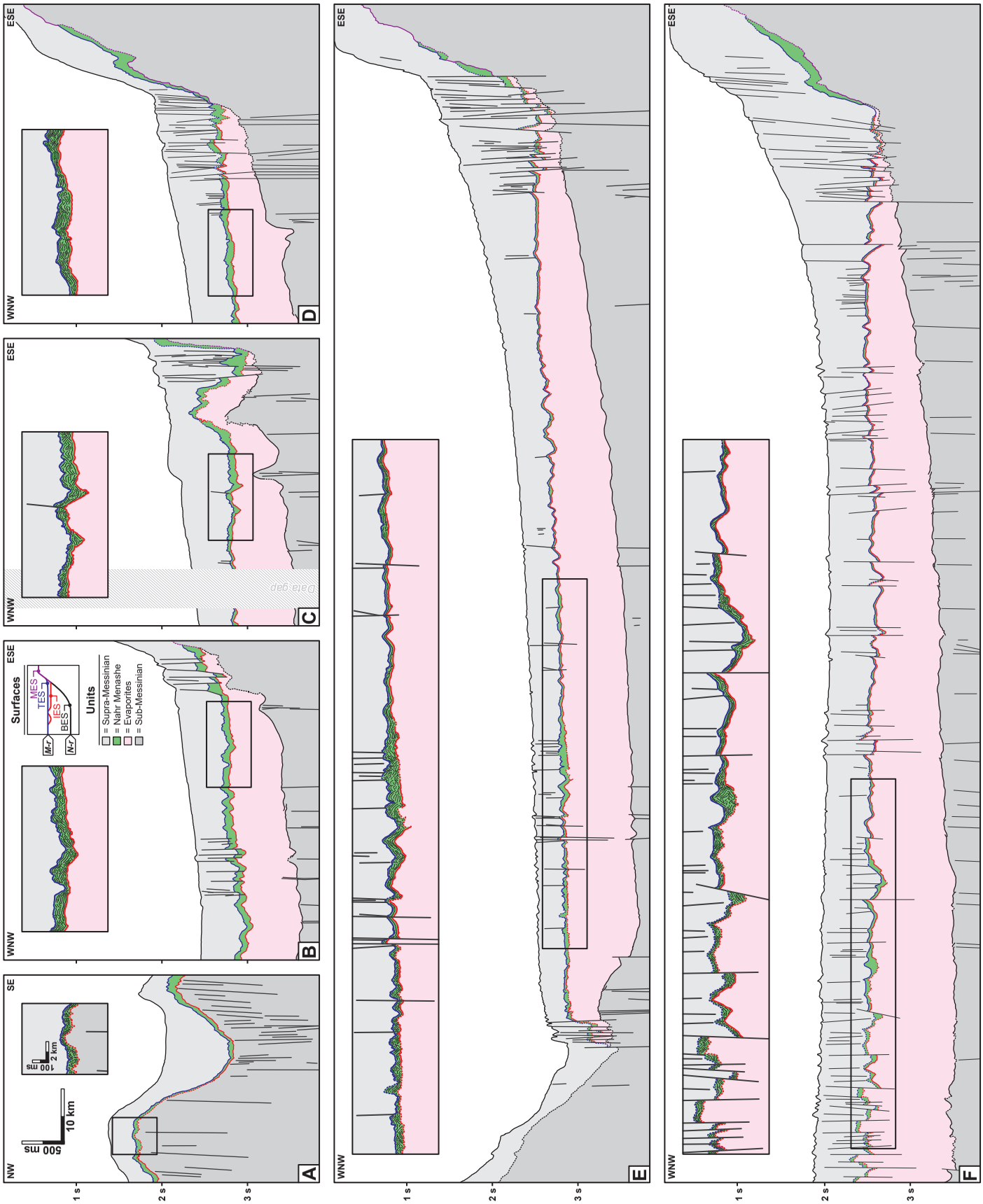

Figure DR2. Interpreted 2D seismic lines (see Fig. DR1 for uninterpreted sections). The Nahr Menashe deposit (green) is a relatively thin accumulation that thickens in a northeastward direction and directly overlies evaporitic deposits (pink). See Fig. 3A (bottom right) for location map; scales are the same for all panels.

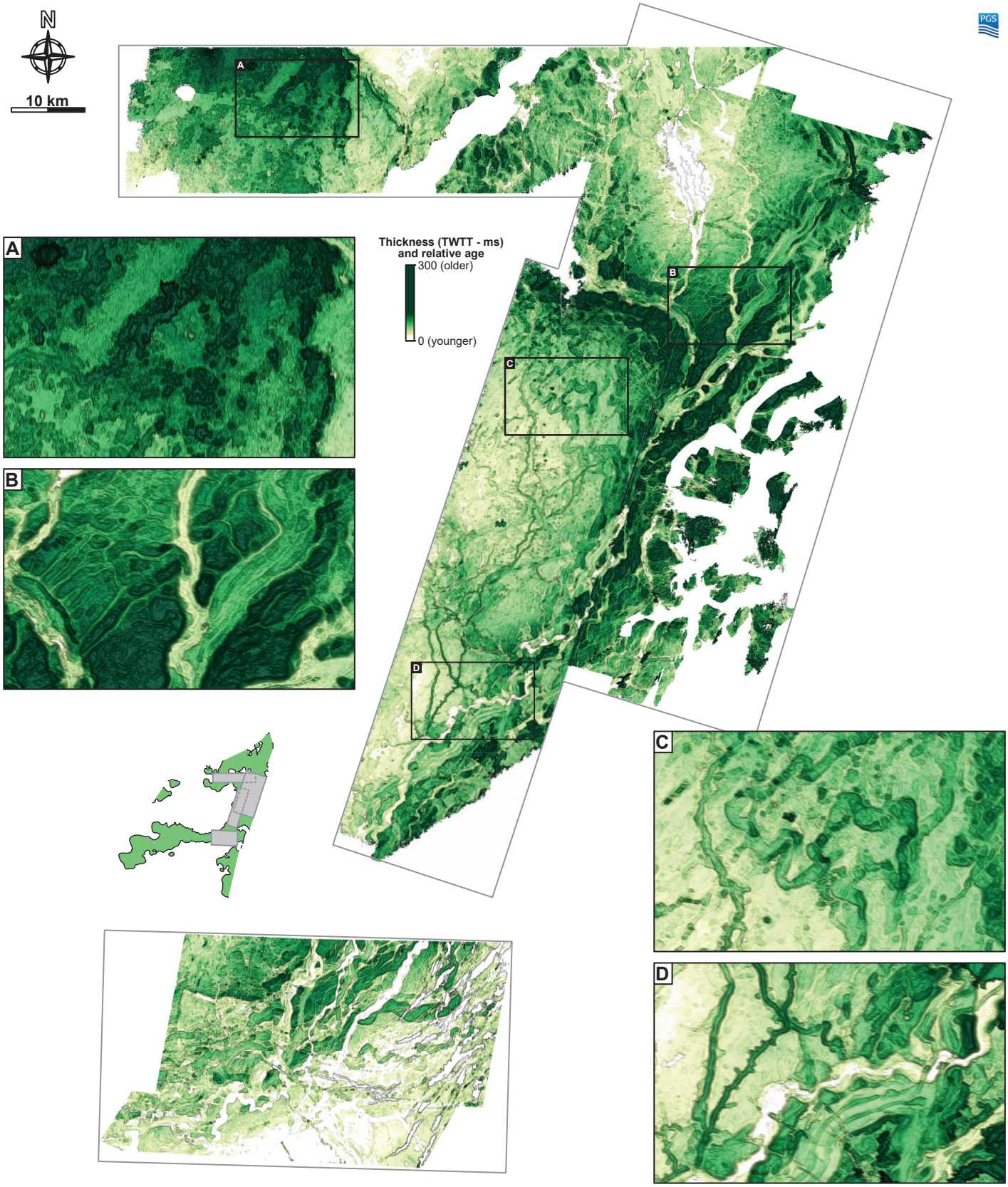

Figure DR3. Uninterpreted isochron map (created from 3D data) showing distribution of thicknesses (in two-way traveltime – TWTT) for the updip Nahr Menashe deposit. The accumulation displays topographic inversion (i.e., erosion-resistant deposits that undergo elevation reversals), with thicker/older accumulations (dark green) occupying higher elevations, and thinner/younger deposits (white) displaying the opposite trend. See Fig. 3A (bottom right) for location map, and Fig. DR5 for interpretation. Data courtesy of PGS and the Lebanese Ministry of Energy and Water.

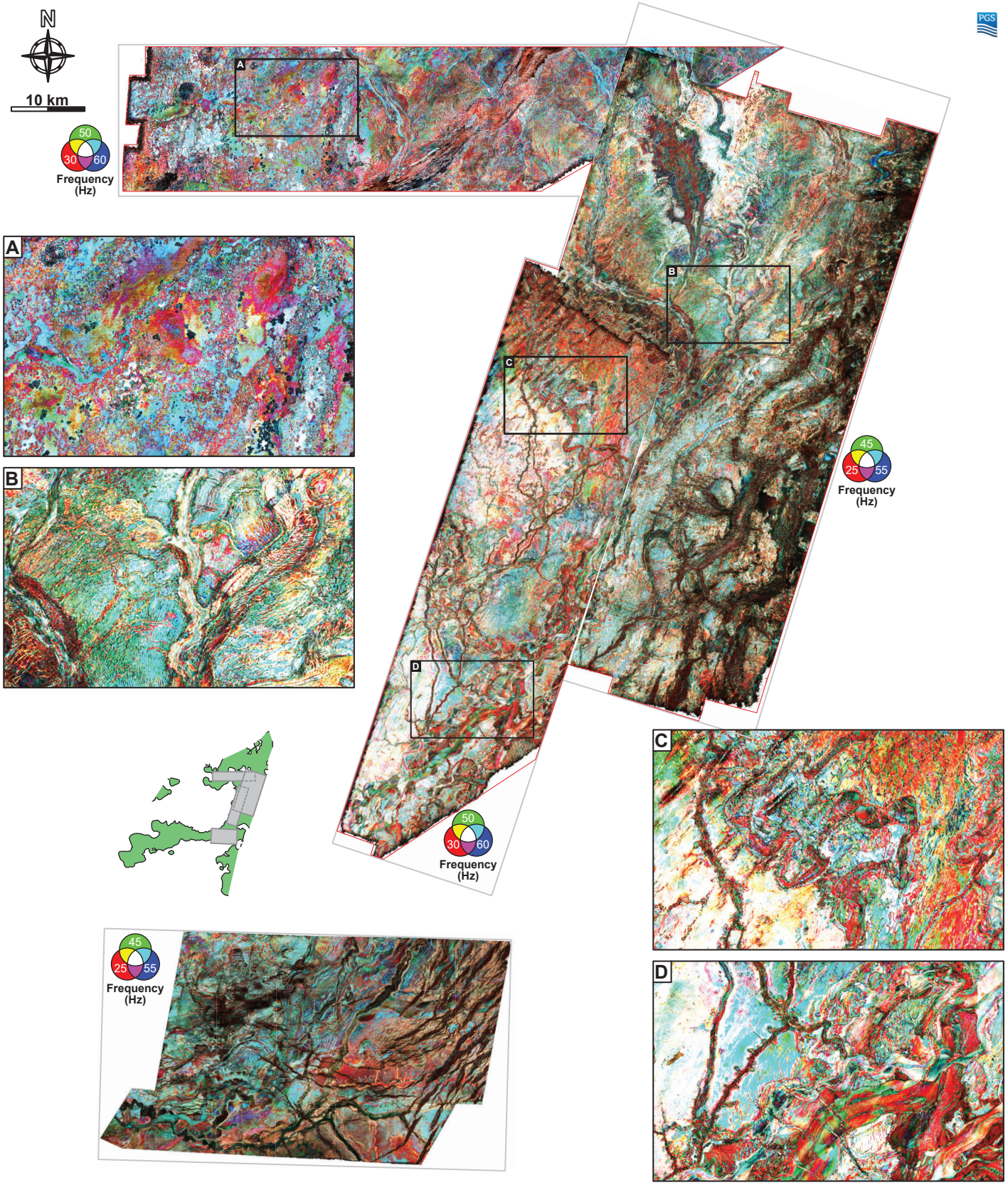

Figure DR4. Uninterpreted spectral decomposition (created from 3D data) showing lateral distribution of seismic frequencies for the updip Nahr Menashe deposit. Thicker/more homogeneous accumulations are displayed in warmer colors (lower frequencies), whereas thinner/more heterogeneous deposits are shown in cooler colors (higher frequencies). See Fig. 3A (bottom right) for location map, and Fig. DR5 for interpretation. Data courtesy of PGS and the Lebanese Ministry of Energy and Water.

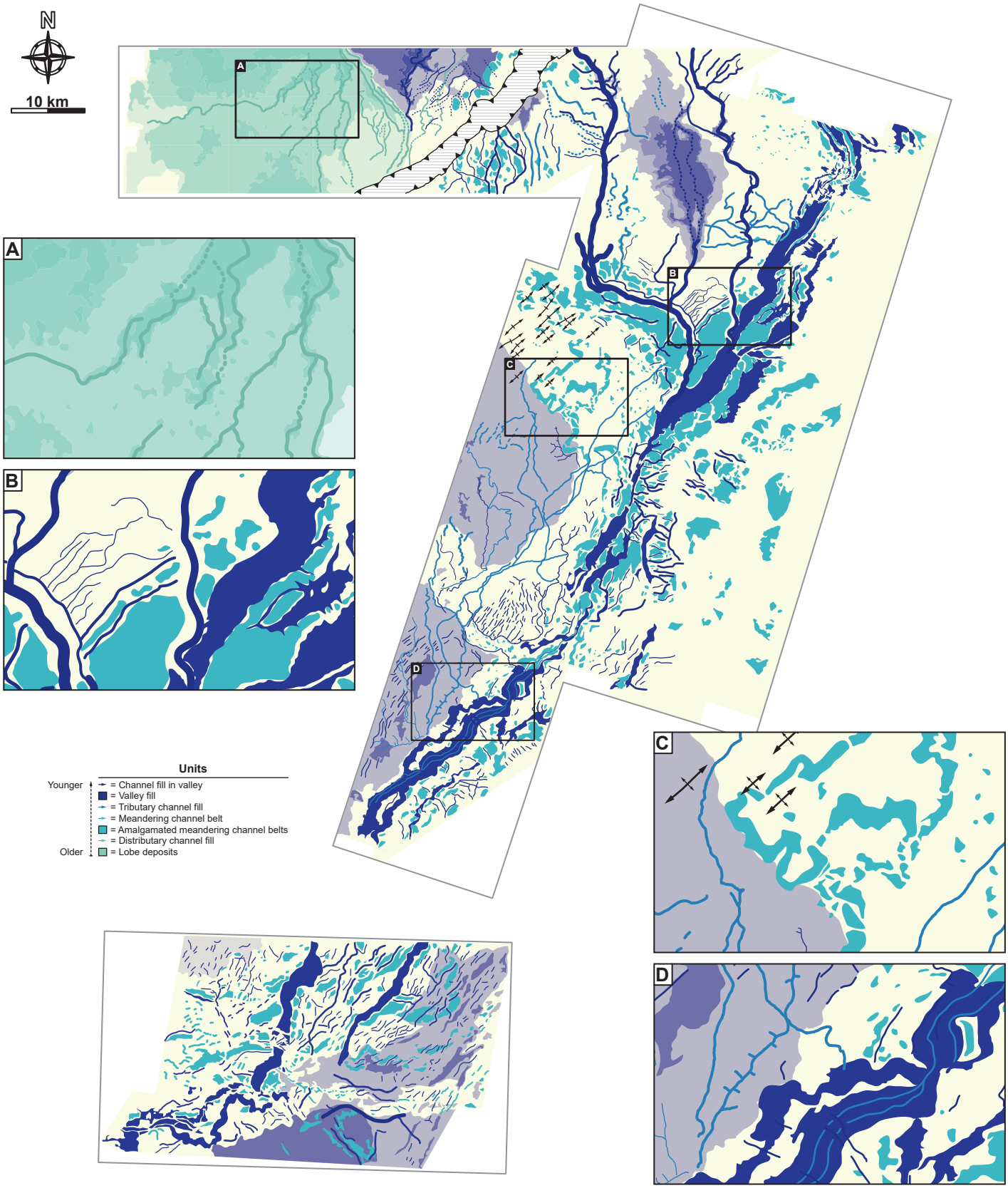

Figure DR5. Simplified geologic map of the updip Nahr Menashe deposit, showing distribution of non-marine facies. Note the presence of valley fill, channel belts, and lobes. See Figs. DR4 and DR5 for uninterpreted maps.

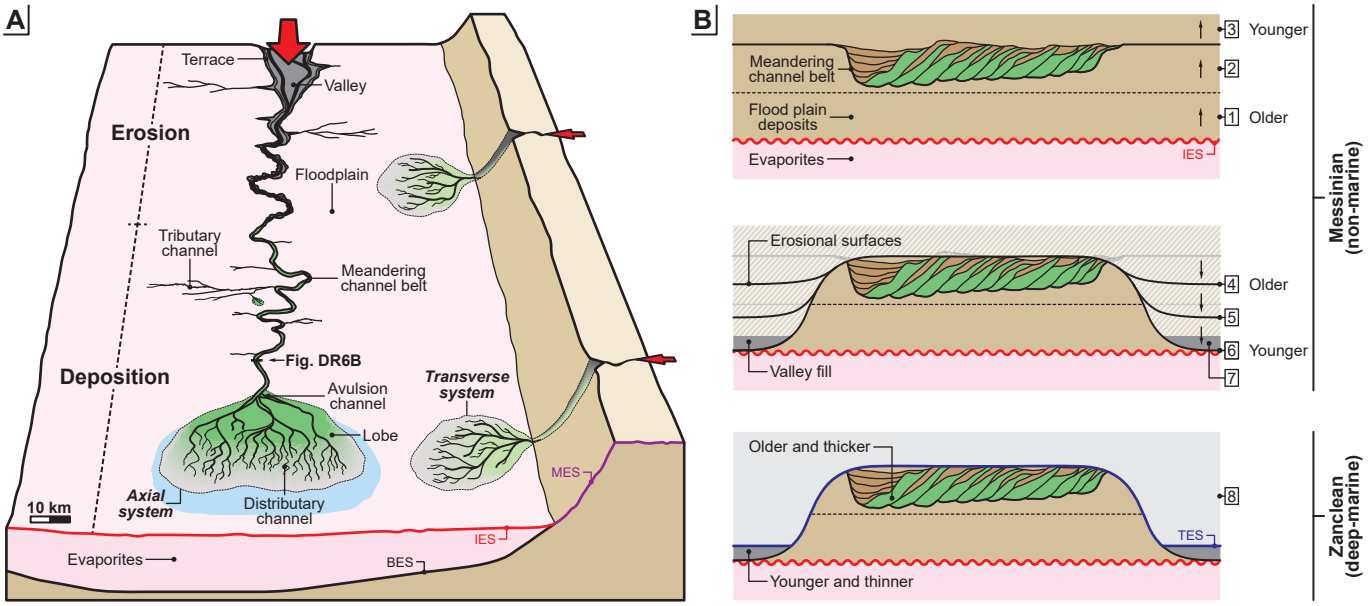

Figure DR6. Aggradational and degradational models for the Nahr Menashe deposit (compare to Fig. 3A). A: The accumulation consists of axial and transverse fluvial deposits, with the former following the regional gradient (i.e., longer run-out distance) and the latter constrained by the local base-of-slope (i.e., shorter run-out distance). Red arrows indicate sediment-transport directions. B: Post-depositional topographic inversion. Deposits accumulate directly over evaporites (times 1-3 – top), with porous fluvial sediments undergoing early cementation. Topographic inversion develops via the successive downcutting of fluvial terraces and valleys (times 4-6 – middle), leaving coarser/more cemented deposits at higher elevations. At lower positions, remobilized and finer/less cemented non-marine sediments fill fluvial valleys (time 7 – middle). Subsequent to marine transgression, deep-water accumulations onlap inverted deposits (time 8 – bottom); compare to Fig. 3A – inset A1.

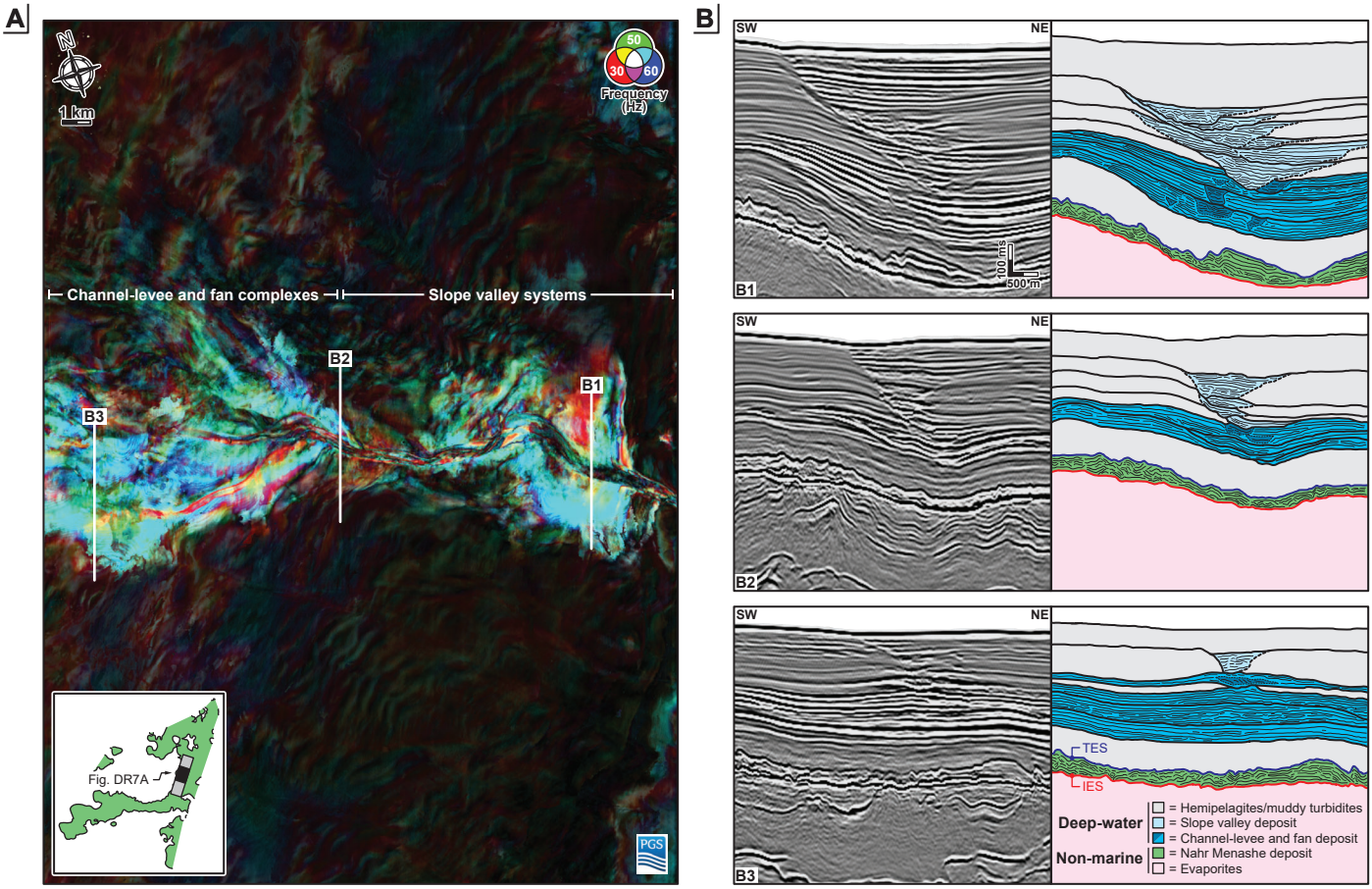

Figure DR7. Comparison of the seismic stratigraphy of a Plio-Pleistocene deep-water accumulation to the underlying Nahr Menashe deposit. A: Spectral decomposition (created from 3D data) showing lateral distribution of seismic frequencies of a deep-water accumulation; the deposit transitions basinward (westward) from slope valleys (i.e., erosionally confined) to channel-levees (i.e., aggradationally confined) to fans (i.e., unconfined). B: Interpreted seismic sections showing deep-water accumulation (blue) and underlying fluvial Nahr Menashe deposit (green); the former is significantly thicker and displays less internal lateral variability than the latter. The younger deep-water accumulation is interpreted to have flowed perpendicular to the Nahr Menashe deposit. Data courtesy of PGS and the Lebanese Ministry of Energy and Water.